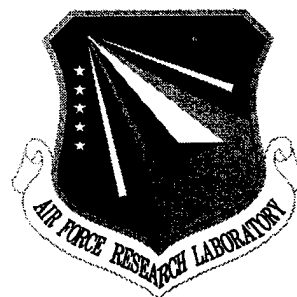AFRL-SN-RS-TR-1999-261
Final Technical Report
January 2000

# RECIRCULATING PHOTONIC FILTER (RPF): A WAVELENGTH SELECTIVE TRUE TIME DELAY FOR OPTICALLY CONTROLLED PHASED ARRAY SENSORS

University of California, Los Angeles

Sponsored by
Defense Advanced Research Projects Agency
DARPA Order No. A0-E391

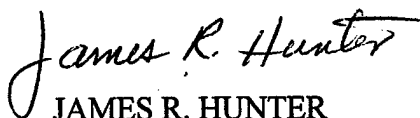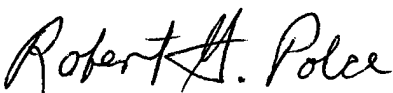*APPROVED FOR PUBLIC RELEASE; DISTRIBUTION UNLIMITED.*

20000214 066

AIR FORCE RESEARCH LABORATORY
SENSORS DIRECTORATE
ROME RESEARCH SITE
ROME, NEW YORK

DTIC QUALITY INSPECTED 1

This report has been reviewed by the Air Force Research Laboratory, Information Directorate, Public Affairs Office (IFOIPA) and is releasable to the National Technical Information Service (NTIS). At NTIS it will be releasable to the general public, including foreign nations.

AFRL-SN-RS-TR-1999-261 has been reviewed and is approved for publication.

APPROVED: *James R. Hunter*

JAMES R. HUNTER
Project Engineer

FOR THE DIRECTOR: *Robert H. Polce*

ROBERT G. POLCE, Chief
Rome Operations Office
Sensors Directorate

# RECIRCULATING PHOTONIC FILTER (RPF): A WAVE-LENGTH SELECTIVE TRUE TIME DELAY FOR OPTICALLY CONTROLLED PHASED ARRAY SENSORS

Bahram Jalali

# REPORT DOCUMENTATION PAGE

*Form Approved*
*OMB No. 0704-0188*

| 1. AGENCY USE ONLY *(Leave blank)* | 2. REPORT DATE | 3. REPORT TYPE AND DATES COVERED |
|---|---|---|
| | January 2000 | Final    Nov 96 - Aug 98 |

**4. TITLE AND SUBTITLE**

RECIRCULATING PHOTONIC FILTER (RPF): A WAVELENGTH SELECTIVE TRUE TIME DELAY FOR OPTICALLY PHASED ARRAY SENSORS

**6. AUTHOR(S)**

Bahram Jalali

**5. FUNDING NUMBERS**

C - F30602-97-C-0019
PE - 63765E
PR - E391
TA - 00
WU - 01

**7. PERFORMING ORGANIZATION NAME(S) AND ADDRESS(ES)**

University of California, Los Angeles
10945 LeConte Ave/1400 PVUB
Los Angeles, CA 90095-1406

**8. PERFORMING ORGANIZATION REPORT NUMBER**

N/A

**9. SPONSORING/MONITORING AGENCY NAME(S) AND ADDRESS(ES)**

Defense Advanced Research Projects Agency    AFRL/SNDR
3701 North Fairfax Drive    25 Electronic Pky
Arlington VA 22203-1714    Rome NY 13441-4515

**10. SPONSORING/MONITORING AGENCY REPORT NUMBER**

AFRL-SN-RS-TR-1999-261

**11. SUPPLEMENTARY NOTES**

AFRL Project Engineer: James R. Hunter/SNDR/(315) 330-7045

**12a. DISTRIBUTION AVAILABILITY STATEMENT**

Approved for Public Release; Distribution Unlimited.

**12b. DISTRIBUTION CODE**

**13. ABSTRACT** *(Maximum 200 words)*

This report describes out theoretical investigation into the nature of the experimentally observed loss and crosstalk in the RPF. The study shows that the loss of the RPF can be reduced to around 2dB through optimum design of the diffraction grating and waveguide. Phase linearity and measurements and temperature sensitivity of the RPF are also presented. We then describe optically-controlled two-dimensional beam-steering systems wherein the signal is transferred between the delay states all-optically be employing wavelength conversion in a semi-conductor optical amplifier (SOA). We describe the concept and demonstrate experimentally this scheme to achieve independent control of azimuth and elevation beam steering. Applications of this technique include the ability to extend the total number of discrete time delays. In any wavelength-selective time-delay technique the spectral tuning range of the tunable laser source limits the number of different delays that can be obtained. However, by cascading two N-channel time-delay stages with wavelength conversion, we now obtain N2 different delays. Another application is the ability to realize digitally controlled time-delays. An m-stage cascade, with m-independently tuned lasers, can be used to realize the most significant bit (MSB) while the successive time-delay stages will represent the less significant bits.

**14. SUBJECT TERMS**

Photonic True Time Delay, Photonic Filter, Optical Processing, Optical Control of Phased Arrays

**15. NUMBER OF PAGES**

32

**16. PRICE CODE**

| 17. SECURITY CLASSIFICATION OF REPORT | 18. SECURITY CLASSIFICATION OF THIS PAGE | 19. SECURITY CLASSIFICATION OF ABSTRACT | 20. LIMITATION OF ABSTRACT |
|---|---|---|---|
| UNCLASSIFIED | UNCLASSIFIED | UNCLASSIFIED | UL |

# TABLE OF CONTENTS

# TABLE OF FIGURES

# 1.0 Abstract

This report constitutes the final report on the DARPA funded Recirculating Photonic Filter (RPF) contract. It describes our theoretical investigation into the nature of the experimentally observed loss and crosstalk in the RPF. The study shows that the loss of the RPF can be reduced to around 2dB through optimum design of the diffraction grating and waveguide. Phase linearity and measurements and temperature sensitivity of the RPF are also presented We then describe optically-controlled two-dimensional beam-steering systems wherein the signal is transferred between the delay stages all-optically by employing wavelength conversion in a semi-conductor optical amplifier (SOA). We describe the concept and demonstrate experimentally this scheme to achieve independent control of azimuth and elevation beam steering.

Applications of this technique include the ability to extend the total number of discrete time delays. In any wavelength-selective time-delay technique the spectral tuning range of the tunable laser source limits the number of different delays that can be obtained. However, by cascading two N-channel time-delay stages with wavelength conversion, we now obtain $N^2$ different delays. Another application is the ability to realize digitally controlled time-delays. An m-stage cascade, with m-independently tuned lasers, can be used to realize $2^m$ independent delays which can be set by an m-bit parallel control word. The first time-delay stage would be used to realize the most significant bit (MSB) while the successive time-delay stages will represent the less significant bits.

# 2.0 Project Overview

This section provides an overview of the project. The objective of this project was to realize a compact, reliable and affordable true time delay technology. Currently, there is considerable interest in employing optical control of phased array sensors. This stems mainly from the broadband nature of optical time delays that prevents beam squint. Our approach uses a phased-array waveguide grating and can be readily integrated on a single substrate using the silica or semiconductor waveguide technology. The new integrated true-time-delay (TTD) technology is monolithic and can be manufactured using silicon integrated circuit processing.

In the proposed device shown in Figure 1, the TTD is obtained by the RPF consisting of an optical phased-array waveguide grating in a symmetric feedback configuration. The latter is depicted in Figure 2. In transmit and receive mode, the r.f. modulated optical carrier is steered by the waveguide grating to the appropriate integrated delay line depending on the carrier wavelength. The signal is delayed and
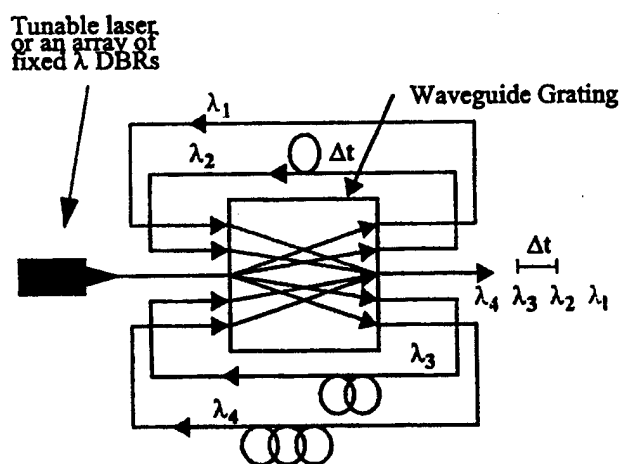


**FIGURE 1.** The Recirculating Photonic Filter (RPF). B. Jalali and S. Yegnanrayanan, US Patent No. 5,793,907.

1

is fed back into the symmetric input port. The grating then diffracts the delayed beam into the common output port.

The RPF has several advantages over other wavelength selective TTD techniques. It is a two port device. Hence, it eliminates the need for optical circulators required in other approaches based on the Bragg grating. The routing and time delay functions are integrated on a single piece of silicon, leading to reliability and affordability. The device loss is independent of the number of delay channels, hence it can be readily scaled to large antenna arrays.

The prototype RPF TTD has been realized by using an eight-channel waveguide grating with 0.8nm channel spacing and 6.4nm free spectral range. The device is based on the silica waveguide technology and operates in the 1550nm wavelength range. The total optical insertion loss for each wavelength channel is ~6dB. The crosstalk for the waveguide grating is ~27dB optical, corresponding to ~54dB electrical isolation. The results clearly demonstrated the ability of the RPF to generate true time delays which are dependent on the wavelength of the optical carrier. Further, as expected, the delay was shown to be independent of r.f. frequency (see Figure 3).
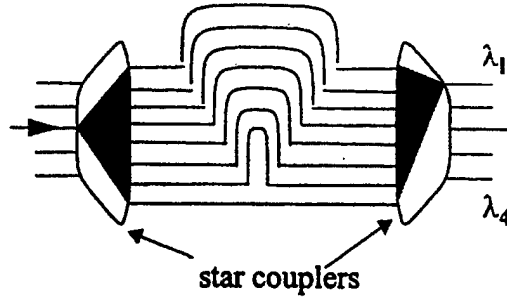
**FIGURE 2.** The waveguide grating used for signal routing in the RPF. The RPF consists of the waveguide grating in a recirculating configuration.
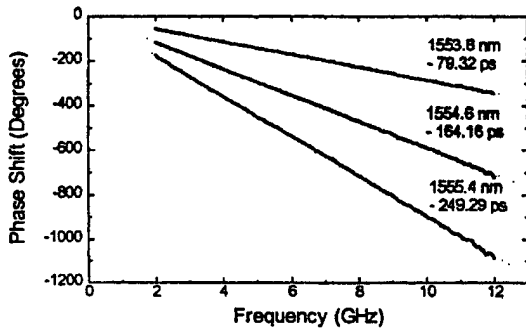
**FIGURE 3.** Measured r.f. phase Vs. frequency curves for various optical wavelengths. The data shows the ability to switch the r.f. time delay by changing the optical wavelength. Further, the delay (slope) is independent of r.f. frequency.

An important and unique property of the RPF is its broadband operation. The electrical bandwidth of the RPF, defined as the 3dB width of the passband, is approximately 37GHz. In a previous report it was shown that the RPF can operate at both 1.3 and 1.55μm wavelength bands. This property is unique and is markedly different than the narrow band operation of fiber bragg gratings.

## 3.0 Study of Loss

Our goal was to develop an understanding of the physical origin of loss and investigate possible methods of improving it.

There are three main loss contributions.

The first is the loss in the input star coupler. The input beam diffracts in the star coupler. However, only a fraction of the diffracted power is captured by the grating waveguides (see

2

Figure 4). The loss is determined by the aperture of the grating waveguides compared to the diffracted beam width and can be reduced to as low as 0.2dB.

The second contribution to the loss arises from the diffraction loss at the second star coupler at the output. Here, the optical signals from each of the grating waveguides interferes, very similar to a diffraction grating. The beam is diffracted into the designed grating order m, but also into various higher and lower grating orders (see Figure 5). The power diffracted into the desired grating order m, represents the collected power at the output, whereas the power diffracted into all the other grating orders represents diffraction loss. The strength of the scattering into each grating order is determined by the diffraction pattern envelope. We can easily see that this diffraction pattern envelope is simply determined by the diffraction from a single waveguide. A small waveguide mode results in large diffraction loss. Figure 6 shows the diffraction efficiency as a function of the dimensionless parameter $w_o/d$, where $w_o$ is the waveguide mode size and d is the grating pitch.

The larger the optical mode, the more efficient the diffraction grating scatters into the desired grating order. However, as the optical mode becomes comparable to the grating pitch, the adjacent grating waveguides experience crosstalk, which induces both amplitude and phase front non-uniformities which can cause significant aberration. A diffraction efficiency of around

**FIGURE 4.** **Input Optical Star Coupler. Loss due to finite aperture of grating waveguides.**
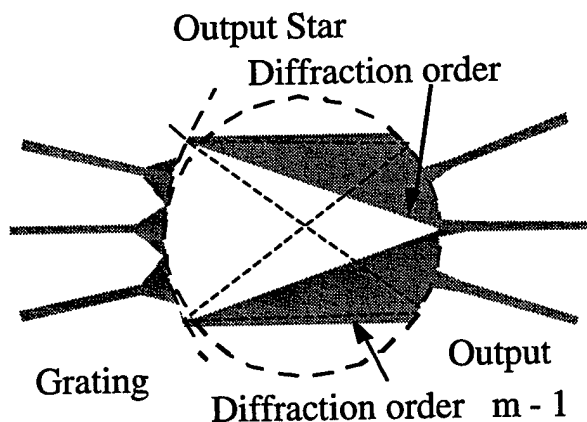
**Figure 5: Output Optical Star Coupler. Loss due to scattering to higher/lower diffraction orders.**
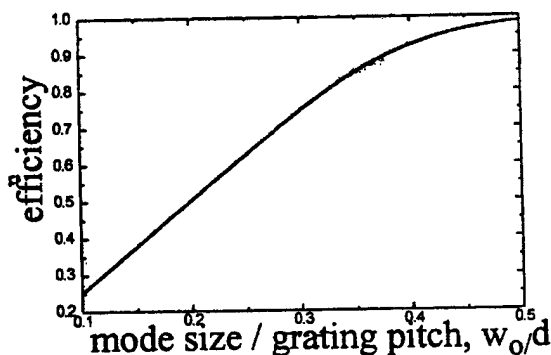
**FIGURE 6.** **Output Diffraction efficiency as a function of waveguide mode size.**

70% achieves reasonable compromise between diffraction efficiency waveguide crosstalk. This results in a diffraction loss at the output star coupler of ~1.5dB.

The third contribution to the loss arises from the finite propagation loss in the waveguide. Silica glass waveguides exhibiting as low as 0.01dB/cm propagation loss have been reported

while <0.1dB/cm loss glass waveguides are available commercially. Nevertheless, the total propagation loss can be ~2dB. The fourth contribution to the loss arises from the coupling loss at the input from fiber to waveguide and similarly at the output between the waveguide and fiber. Due to the fact that the glass waveguides are low-index contrast waveguides, with refractive index and mode size closely matched to the optical fiber, this coupling loss can be reduced to ~0.2dB. The conclusion from the loss analysis is that it is realistic to expect an overall loss of approximately 3.7dB from fiber to fiber. Presently, the loss is of the order of 5-6dB. Hence, there exists scope for improvement of the insertion loss of the RPF.

## 4.0 The Study of Crosstalk

This section reports on the nature of crosstalk in the RPF. The experimentally measured crosstalk for the prototype device available in our lab is –27dB optical corresponding to –54dB electrical isolation. Our goal was to develop an understanding of the physical origin of crosstalk and investigate possible methods of improving it.

The key to understanding the crosstalk is optical interference in the second star coupler (see Figure 7).

The input star coupler functions to diffract the incident optical energy into the grating waveguides, thereby determining the "strength" of each grating waveguide radiator. Any two adjacent grating waveguides have the same path length difference $\Delta L$. This introduces a phase difference of $2\pi n\Delta L/\lambda$ across the grating waveguides, where n is the effective refractive index of the waveguide. The light emitted from the grating waveguides is then diffracted at an angle $\theta$ which satisfies

$$n\Delta L + nd\sin\theta = m\lambda$$

where d is the pitch of the grating and m is the diffraction order. This diffracted beam can also be understood as the direction of constructive interference when the radiation from all the waveguide grating radiators are in phase.

*Grating Waveguides*        *Interference Pattern*

**FIGURE 7.** Optical phased-array operation in the second star coupler of the RPF. The interference sidelobes contribute to the inter-channel crosstalk.

Borrowing from antenna theory, this array is then analogous to a phase scanning antenna array. This interference pattern is shown in Figure 7. Notice that in addition to the main lobe we have well-defined, albeit much lower, energy in the side-lobes as well. This represents optical crosstalk. Why is this crosstalk important for the RPF? Since we are actually folding all outputs to achieve the wavelength dependent time delay, even the crosstalk gets folded over. However, the crosstalk is delayed by a different time delay and this results in phase excursions for the radio frequency sub-carrier from the desired linear phase-frequency response for true-time delay operation.

4

To understand the nature of the optical crosstalk we have used a simple model for the output waveguide grating. The transmission spectrum between input port p and output port q (p,q=-N/2..N/2), for an N channel grating with M waveguides in the grating section, having a grating excitation coefficient $\gamma_k$ (k=0,1,2,3,..M-1) for the amplitude of each waveguide grating radiator, is simply given by the absolute square of the frequency response

$$H(\lambda) = \sum_{k=0}^{M-1} h_k(\lambda)$$

Where $h_k(\lambda)$, the field at $k$ th grating waveguide is

$$h_k(\lambda) = \gamma_k \exp\left(ik\frac{2\pi}{\lambda}n\Delta L\right)\exp\left(ik\frac{2\pi}{\lambda}nR\theta_{in}\theta_{out}(p-q)\right)$$

Where $R\theta_{in}=\Delta x$ and $R\theta_{out}=d$. If we assume a random optical path phase error of $\varepsilon_k$ (k=0,1,2,3,..M-1) then the frequency response is given by

$$H(\lambda) = \sum_{k=0}^{M-1} g_k(\lambda) \qquad g_k(\lambda) = h_k(\lambda)\exp(i\varepsilon_k)$$

Where, the field at the $k$ th grating waveguide is modified by the random phase error exp $(i\varepsilon_k)$.

We have used this model to study the effect of the grating parameters such as number of waveguides in grating, and also the presence of lithography limited random optical path phase error in grating waveguides on the obtained optical crosstalk. This theoretical investigation also offers insight into the nature of the experimentally observed crosstalk in the RPF. All simulations assume a Gaussian distribution for the grating excitation coefficient $\gamma_k$ which is determined by the input star coupler radius, grating waveguide spacing ($R\theta_{in}=\Delta x$) and the waveguide mode size $\omega_0$ through the relation

$$\gamma_k(\lambda) = \exp\left[(-2)\left(\frac{2\pi}{\lambda}n\omega_0\theta_{in}\right)^2\left(k-\frac{M}{2}-p\right)^2\right]$$

The parameters of the silica waveguide grating we studied is listed below

    W = 8 μm
    N = 1.4529
    ΔL = 252 μm
    Δx = d = 25 μm
    R = 4710 μm
    N = 8 (Number of Channels)
    Δλ = 0.8 nm (100GHz)

Figure 8 shows the intensity transmission spectrum between ports p=0, q=0 with M=8 waveguides in the grating section.

With an increase in the number of grating waveguides we find a reduction in the optical crosstalk. We present in Figure 9 the results with M=40 grating waveguides. A significant
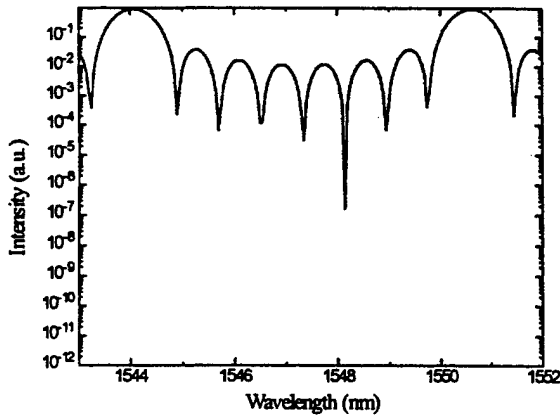


**FIGURE 8.** Optical Transmission Spectrum with M=8 grating waveguides.
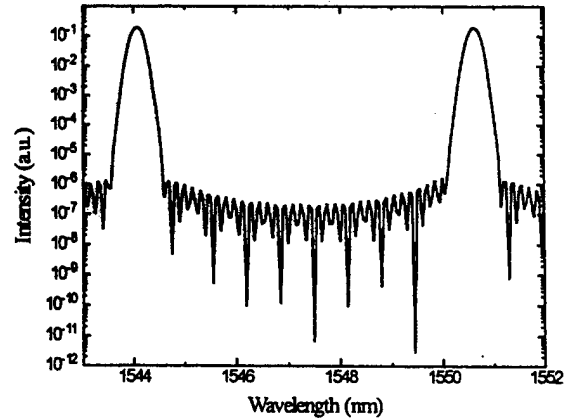


**FIGURE 9.** Optical Transmission Spectrum with M=40 grating waveguides.

reduction in optical crosstalk is clearly observed. This can be understood since the increase in the grating waveguides results in better cancellation of out-of-band signals.

These simulations suggest that with continuous increase in the number of grating waveguides we should continually improve the optical crosstalk. But, this is not observed in reality and the reason is that we have an unavoidable lithography limit which introduces random path length errors in the grating waveguides. Figure 10 shows the effect of random path length phase error on the crosstalk performance of the RPF. The effect of random path length phase error is to introduce a floor to the optical crosstalk that cannot be improved by further increase in grating waveguides.

For a 0.01 μm random path length error this results in a –30dB optical crosstalk floor assuming M=30 grating waveguides.

In summary, this study shows that the crosstalk decreases with the number of waveguides in the grating section of the RPF. The physical origin of this behavior is identical to that in a phased array antenna where the sidelobe suppression is improved with an increase in the number of radiating elements. However, in the RPF, the ultimate crosstalk is limited by the random phase error introduced by the uncertainty in waveguide length. It is shown that a random mask error of 0.1 μm can limit the crosstalk to –30dB (optical).

## 5.0 Phase Response

The experimentally obtained swept-frequency phase response for a monolithic device with 15 channel grating and integrated delay lines, is shown in Figure 11. This device exhibited a poor optical crosstalk performance of 16dB (for the worst channel). The main reason for phase
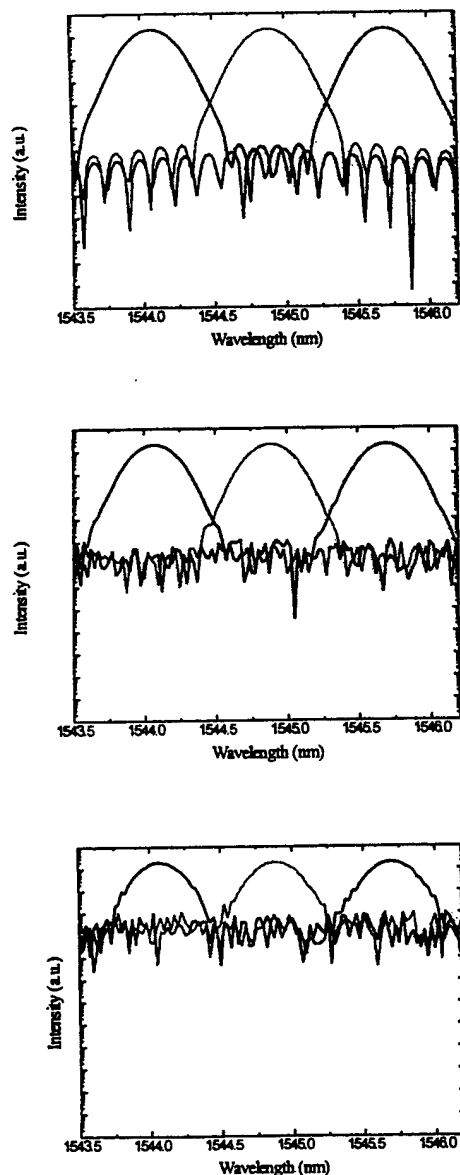
FIGURE 10. Effect of random path length phase error on optical crosstalk performance of grating.(a) Ideal Grating, (b) 0.01 μm random error, and (c) 0.1 μm random error. M=30 for all simulations.
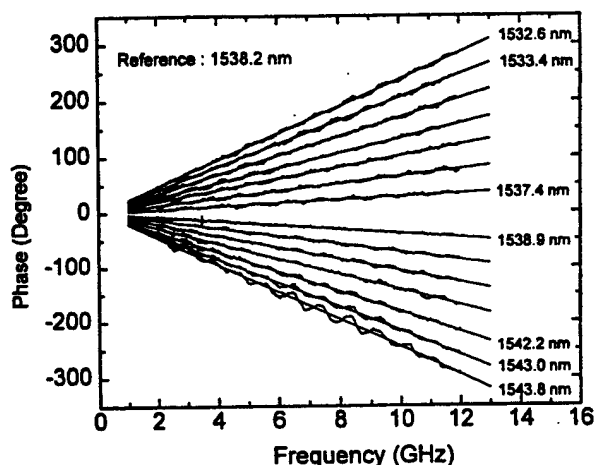
FIGURE 11. Measured swept frequency response for monolithic 15 channel wavelength selective TTD device. Average time delay between adjacent channels is 9.665 ps.

fluctuations is this interchannel crosstalk leading to a small amount of the optical signal leaking into the adjacent undesired waveguide delay lines as shown in Figure 12.

Therefore, at the output of the recirculating photonic filter, we have the desired electrical signal and several undesired signals that have suffered different time-delay and also have much smaller amplitude compared to the desired signal due to the fact that they are due to optical crosstalk. This causes the electrical phase of the resultant signal to oscillate around the selected linear variation as we sweep the RF frequency. The predicted swept-frequency measurements using this phase response model agrees with the experimental measurements. Since the optical crosstalk is the primary reason for phase variations, one can estimate the crosstalk value that satisfies system requirements for phase linearity. Anticipated linearity requirements are

+/- 4 degrees over the operating frequency band. Hybrid RPF TTD devices with optical crosstalk of 27dB are readily able to meet this phase linearity requirement as shown in Figure 13.
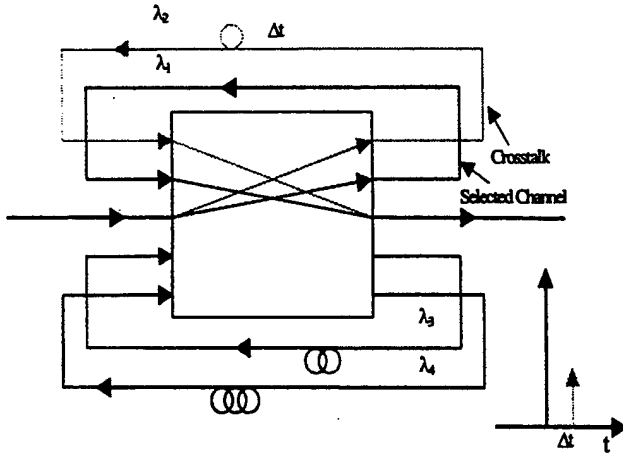


**FIGURE 12.** Phase response model. Crosstalk gives rise to time delayed and attenuated versions of the signal.
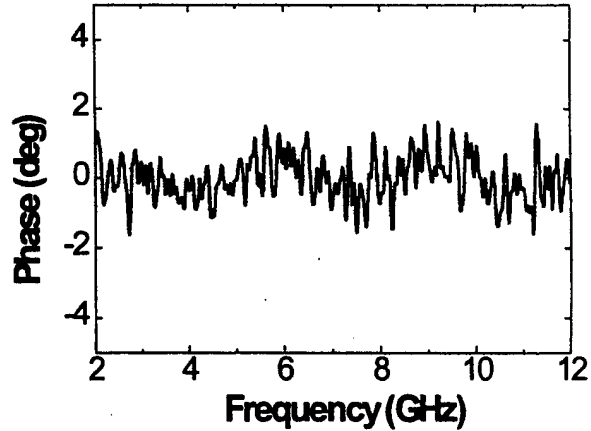
**FIGURE 13.** Swept frequency phase-linearity measurements. +/- 2 degrees phase variation over the measured 12GHz bandwidth is observed.

## 6.0 Thermal Stability

The stability of the recirculating photonic filter passband with respect to temperature variations is a critical issue and must be evaluated. Temperature induced shift in the passband frequency arises primarily due to the temperature dependence of the refractive index which may be approximated to first order by the following linear dependence

$$\frac{df}{dT} = \frac{c}{n_c^2 \lambda} \frac{dn_c}{dT}$$

For the best silica-based waveguide technology, the temperature coefficient of refractive index is $1 \times 10^{-5}/^0C$, resulting in a thermal shift of approximately $1.03GHz/^0C$. The silica based waveguides exhibit excellent thermal stability. For applications that require stability in extreme temperature condition, the recirculating photonic filter true-time delay device substrate can be temperature controlled using thermoelectric elements. Figure 14 shows temperature tuning measurements. Due to the relatively weak
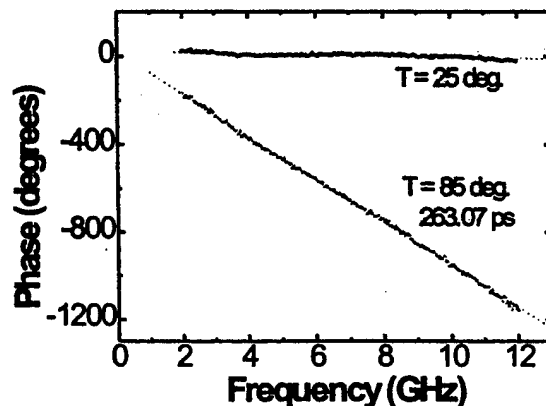


**FIGURE 14.** Thermal stability of the selected time delay. The chip temperature was changed by 60 degrees to select the adjacent channel.

8

thermal effect, a temperature tuning of 60 degrees is required to tune to the adjacent channel (100GHz spacing) of the time-delay device.

## 7.0 Dual Band Operation

In this section we analyze and also demonstrate the broad optical bandwidth of the RPF TTD device. In the optical fiber, the 1550 nm wavelength region is preferred because of the low optical loss and the possibility of using erbium doped fiber amplifiers to compensate for the link loss. The 1300 nm wavelength region is important since the first order group velocity dispersion term is zero in standard single-mode fiber. It would be desirable to be able to operate the same RPF TTD device in both of these wavelength windows to obtain flexibility in system design and enhanced antenna functionality.

The operation of the waveguide prism is dependent on the grating equation. For the case of the center wavelength channel, this equation reduces to $n_c\Delta L = m\lambda$, where $n_c$ is the refractive index of the channel waveguides, $\Delta L$ is the path length difference, $\lambda$ is the center wavelength and m is the grating order. Neglecting refractive index dispersion, the reduction of the center wavelength from 1550nm to 1300nm results in an increase in the grating order m. Hence, the free-spectral range (FSR) given by $\lambda/m$ will be smaller at 1300nm than at 1550nm. Thus, by designing the waveguide grating at 1550nm to have an FSR larger than the channel bandwidth $N\Delta\lambda$, where N is the number of channels and $\Delta\lambda$ is the channel spacing, one can easily offset this reduction in FSR and obtain complete access to the channel bandwidth at 1300nm also.

The 8 channel waveguide grating had an 0.8nm (100 GHZ) channel spacing and a FSR of 6.4nm in the 1550nm wavelength region. When used in the 1300nm band, the FSR is reduced to 4.5nm thus providing only 7 useful channels with a channel spacing of 0.67nm. The measured optical loss and crosstalk at 1300nm and 1550nm show no changes between the two wavelength regions. Selection of the delay line by tuning optical wavelength in the 1300nm spectral region is shown in Figure 15.
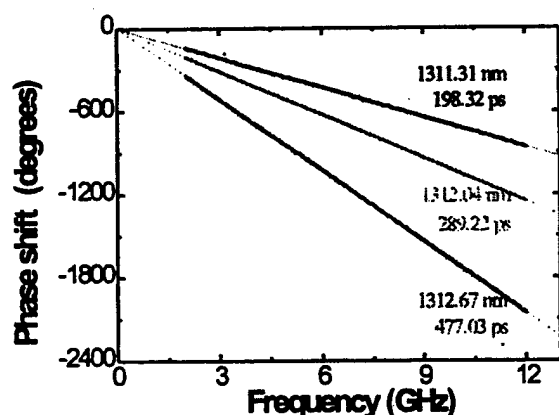


**FIGURE 15. Phase response model. Crosstalk gives rise to time delayed and attenuated versions of the signal.**

## 8.0 Two-Dimensional Beamsteering

In this section we report a technique to extend the RPF time-delay device to real-world two-dimensional beam-steering applications. Other applications of this technique include cascadability of individual time-delay units to achieve dramatic increase in available delays.

Typically one would require a separate photodetector after the first time-delay device followed by an optical modulator to transfer the analog signal to the second time-delay stage. In our technique however, the broadband analog signal is transferred from one waveguide to another without suffering the usual optical-electrical conversion losses.

9

This is achieved by using cross-gain modulation in a semiconductor optical amplifier (SOA) as shown in Figure 16. Since the gain of the SOA saturates with an increase in the optical intensity, an analog signal at $\lambda_1$ modulates the gain of the SOA. A CW beam at $\lambda_2$ samples this
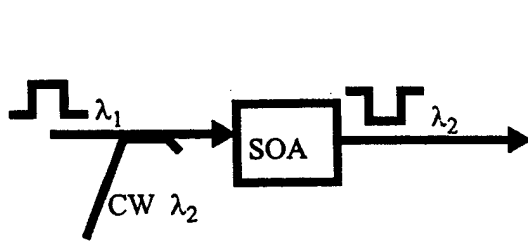


**FIGURE 16.** Broadband Mid-stage Wavelength Translation.
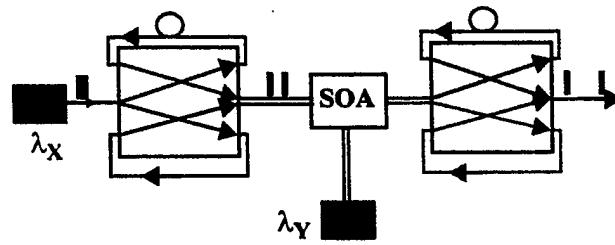


**FIGURE 17.** Cascaded RPF Time-delay Units to achieve Two-dimensional Beam-Steering.

gain modulation, thereby copying the analog signal from $\lambda_1$ to $\lambda_2$.

The maximum frequency of operation is limited only by the simulated emission lifetime, and wavelength conversion at frequencies as high as 20GHz has been demonstrated. Thus, by cascading two individual time-delay devices, each with its own control wavelength, one can set the time delay for the azimuth and elevation to achieve independent two-dimensional optically controlled beam-steering, as shown in Figure 17.

Swept frequency measurements of the RF phase versus RF frequency is shown in Figure 18. The slope of each curve corresponds to the selected RF time-delay. Azimuth laser (11) and elevation laser (12) wavelengths are tuned to select individual time-delays in Figure 18a and Figure 18b. As expected, the time-delay is independent of the microwave frequency over the measured frequency range of 0-6GHz.

In order to verify the wide instantaneous bandwidth of this optical control technique, we performed time-domain measurements using an electrical pulse of 2ns on a 5GHz carrier. The time-domain data in Figure 19 shows one pulse delayed by 70ps with respect to the other, while demonstrating wide instantaneous bandwidth.

Other applications of this technique include the ability to extend the total number of discrete time delays. In any wavelength selective time-delay technique the spectral tuning range of the tunable laser source limits





**FIGURE 18.** (a) Azimuth Laser Tuning (elevation laser set at 1549.6nm) (b) Elevation Laser Tuning (azimuth laser set at 1550nm).

10

the number of different delays that can be obtained. However, by cascading two N-channel time delay stages with wavelength conversion, we now obtain $N^2$ different delays.
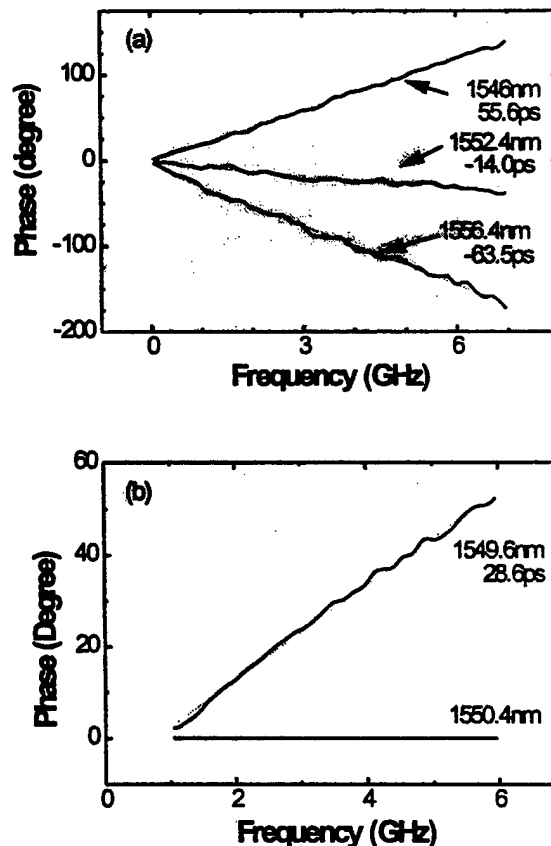
Another application is the ability to realize digitally controlled time-delays. An m-stage cascade, with m-independently tuned lasers, can be used to realize 2m independent delays which can be set by an m-bit parallel control word. The first time-delay stage would be used to realize the most significant bit (MSB) while the successive time-delay stages will represent the less significant bits.
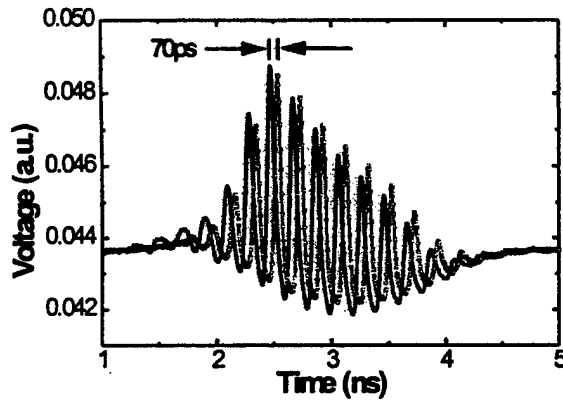


**FIGURE 19.** Time-domain response using 2ns pulsed 5GHz carrier. The response shifts by 70ps when azimuth control wavelength is changed from 1547.6nm to 1553.2nm

## 9.0 Conclusion

In conclusion, we have demonstrated the operation of the recirculating photonic filter (RPF) as an all-optically tunable true-time-delay generator for squint free beam-steering in optically-controlled phased-array antenna. Broad electrical bandwidth operation and optical wavelength control are two of the main features for this device. The study for loss and crosstalk reveals that there is scope for improved performance through suitable device design. One of the fundamental limitations to the insertion loss arises from the finite diffraction loss at the output star coupler. The crosstalk on the other hand has a limit imposed by the finite lithography resolution. However, using existing commercially available devices, we have demonstrated phase linearity that is well within the +/- 4 degree phase excursion stipulated for phased array systems, over the measured bandwidth of baseband to 12 GHz. Cascadability of RPF time-delay stages through inter-stage wavelength translation dramatically increases the number of available delays and achieves two-dimensional beam-steering.

# Appendix A

"Recirculating photonic filter: a wavelength-selective time delay for phased-array antennas and wavelength code-division multiple access"

S. Yegnanarayanan, P.D. Trinh, and B. Jalali

# Recirculating photonic filter: a wavelength-selective time delay for phased-array antennas and wavelength code-division multiple access

S. Yegnanarayanan, P. D. Trinh, and B. Jalali

*Optoelectronic Circuits and Systems Laboratory, Department of Electrical Engineering, University of California at Los Angeles, Los Angeles, California 90095-1594*

A novel wavelength-selective photonic time-delay filter is proposed and demonstrated. The device consists of an optical phased-array waveguide grating in a recirculating feedback configuration. It can function as a true-time-delay generator for squint-free beam steering in optically controlled phased-array antennas and as an encoding–decoding filter for wavelength code-division multiple access.  © 1996 Optical Society of America

Broadband phased-array antennas require true-time-delay devices at each antenna subarray to limit beam squint. Currently, true time delay (TTD) for large-aperture antennas is realized by switched lengths of coaxial cable that are bulky and lossy at high radio frequencies. In addition, switching and control functions become extremely complex, and even low-frequency operation with a large number of antenna element feeds becomes difficult. Optical techniques have been proposed as a potential alternative to improve performance of rf systems for which electromagnetic interference, microwave transmission loss, coaxial cable size and weight, and complex beam forming networks are issue of concern. One can obtain time delay optically by impressing the rf signal onto an optical carrier, which can be delayed in relatively low-loss optical fiber. However, for systems that require a large number of delays the large insertion losses associated with the optical switching network that selects the appropriate delay line are a serious limitation. We propose and demonstrate a photonic filter that uses the optical carrier wavelength to select the desired time delay, thus establishing a one-to-one map between the optical carrier wavelength and the desired antenna direction.

The proposed device also has application in wavelength hopping optical code-division multiple access (CDMA). CDMA is a practicable network control strategy because it overcomes the limitations of switching time associated with optoelectronic devices and the processing delay associated with network protocols. CDMA, however, has its limitations associated with cross talk of its codes and the bandwidth requirements, so optical CDMA has not been a contender in any of the gigabit system test-bed concepts.[1] However, cross-talk limitations in CDMA codes may be reduced through innovative code design, and the bandwidth limitations can be reduced through coding of multiple attributes.[2] Although such multiattribute codes have been proposed for time and space, they can be extended to other waveform attributes, e.g., time and optical wavelength.[1] The recirculating photonic filter (RPF) is ideally suited for performing the function of an optical CDMA encoder–decoder, encoding a data bit in both wavelength and time domains. Such codes

have been shown to increase network security and correlation properties of the codes.[3]

Figure 1(a) shows the proposed integrated-waveguide implementation of the wavelength-selective time-delay function. The concept uses an arrayed-waveguide grating [shown in Fig. 1(b)] in a symmetric feedback (recirculating) configuration. The modulated optical carrier is steered by the waveguide grating to the appropriate integrated delay line, depending on the carrier wavelength. The signal is delayed and is fed back into the symmetric input port. The grating then focuses the delayed beam into the common output port. This TTD can be considered topologically
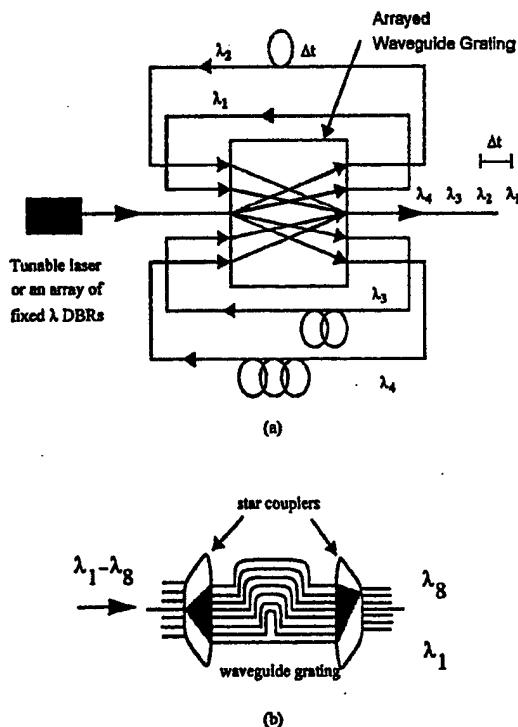


(a)



(b)

Fig. 1.  (a) RPF wavelength-selective TTD.  (b) Schematic of an arrayed-waveguide grating demultiplexer. DBR's, distributed Bragg reflectors.

equivalent to two phased-array waveguide gratings in series with a delay element between. Thus three sequential operations are performed: wavelength demultiplexing, time delay, and wavelength multiplexing. The advantages of the recirculating structure compared with the two devices in series are twofold: the structure occupies roughly one third of a chip area and, more importantly, this configuration ensures that the filters that perform the multiplexing and demultiplexing have identical spectral responses (the same filter does both). Because of inevitable process-related variations, any two devices will have slight variations in their spectral response, rendering the series-connected approach inoperative. It is important to note that the recirculating photonic filter has no $1/N$ loss; all the power at a given wavelength is diffracted into the output port. Furthermore, high resolution (6–8 bits) can be obtained in a compact integrated device.

A prototype RPF TTD device was realized by use of an eight-channel arrayed-waveguide grating demultiplexer with 0.8-nm channel spacing (free spectral range 6.4 nm) whose passband spectrum is shown in Fig. 2. The device is based on silica waveguide technology and operates in the 1.5-$\mu$m wavelength range.[4] The total optical insertion loss for each wavelength channel is ~6 dB. The passband spectrum reveals slightly nonuniform insertion loss and interchannel cross talk. As rf detection and phase information are of concern, small variations in insertion loss suffered by individual wavelength channels are not relevant. However, cross talk could result in pathlength ambiguity in the feedback, resulting in phase error for the rf signal, and needs to be low. The cross talk for arrayed-waveguide grating filters used was ~26 dB; however, values below 30 dB have been reported.[4] Light from an external cavity tunable laser was directly rf modulated at 10–40 MHz and was coupled into the arrayed-waveguide grating chip. Obviously, by using external modulation (e.g., high-speed Mach–Zehnder modulators) one can extend the RPF TTD technique to the microwave and millimeter-wave ranges. The output was detected by an InGaAs p–i–n photodiode, and time–phase measurements were performed with a digital oscilloscope. Input coupling and output coupling were achieved by multifiber ribbons. Feedback delay lines consisted of optical fibers of different lengths connected among four symmetric pairs of input and output ports.

Time delay can be obtained from the slope of the rf phase versus its frequency. The measured data at four different optical wavelengths are shown in Fig. 3. For each measurement the phase of the delayed signal is measured with respect to the center frequency, i.e., the direct path through the device. The delays associated with the direct path, the photodetector, and the electronics are thus canceled, yielding the true delay of the feedback line. The time delays obtained from phase-frequency measurements are 5, 10, 25, and 30 ns for $\lambda$ = 1541.1, 1542.7, 1545.9, and 1544.3 nm, respectively. The approximate lengths of the off-chip fiber feedback lines for these time delays were 0.75, 1.52, 3.8, and 5.5 m, respectively. In a monolithic version, the feedback lines can be integrated on the same chip as the arrayed-waveguide grating. In this

way, subpicosecond incremental delays can be achieved with submicrometer precise delay length. The results clearly demonstrate the ability to use the optical wavelength to switch among various rf time delays. Furthermore, as expected, the delay has the desired property of being independent of rf.

Figure 4 shows one possible implementation of the RPF in a system architecture proposed by Lembo et al.[5] for a parallel fed antenna array. The RPF TTD feeds each subarray, providing a particular delay for a given optical wavelength. The antenna is time-delay steered at the subarray level and phase steered at the element level. The magnitude of time delay
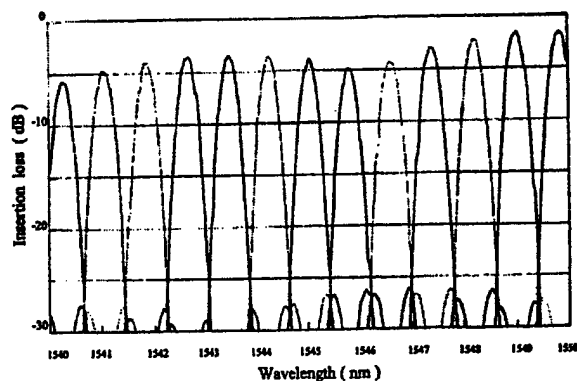


Fig. 2. Passband spectrum of the 8 × 8 arrayed-waveguide grating filter used in the time-delay experiments.
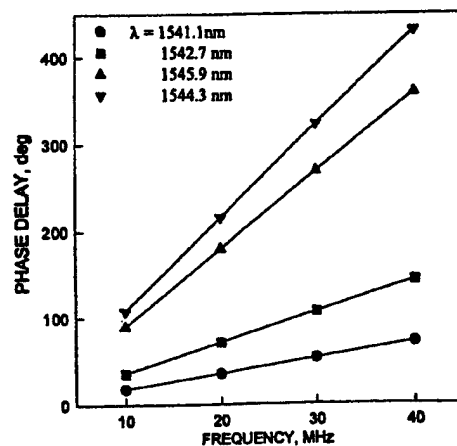


Fig. 3. Measured rf phase delay as a function of rf for four different optical wavelengths.
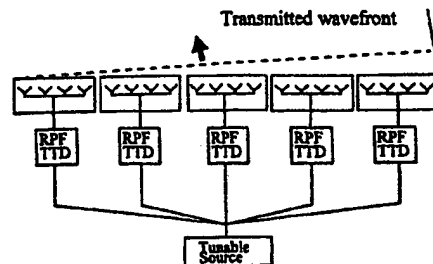


Fig. 4. Use of a RPF in a parallel-fed antenna array similar to that proposed in Ref. 5

depends on the dimension of the phased-array antenna, the maximum steering angle $\theta_{max}$, and the rf. The maximum delay is $(M\lambda_{rf}/2c)\sin\theta_{max}$, where $M$ is the number of elements, $\lambda_{rf}$ is the rf wavelength, and $c$ is the velocity of light. Assuming a rf of 5 GHz, a $72 \times 72$ element array, and a maximum angle of 60°, the maximum delay is 6.24 ns. Typically, the time delay is quantized in units of one rf wavelength with phase shifters providing subperiod control at the subarray level.[5] The total number of discrete time delays is then $(M/2)\sin\theta_{max} \sim 32$, or 5 bits. The total delay corresponds to an ~128-cm length of silica waveguides. Recently silica waveguide delay lines up to 100 cm were demonstrated.[6] Thus it is anticipated that the necessary delay lines can be readily integrated on a single substrate.

The stability of the RPF pass band with respect to temperature variations is a critical issue and must be evaluated. Temperature-induced shift in the passband frequency arises primarily because of the temperature dependence of the refractive index. This can be estimated to a reasonable degree of accuracy by the linear dependence. The temperature dependence of the passband frequency is then given by $df/dT = [c/(n_c^2\lambda)](dn_c/dT)$.

In silica waveguide technology the temperature coefficient of the refractive index is approximately $1 \times 10^{-5}$/°C, resulting in a thermal shift of 1.03 GHz/°C. Thus silica-based waveguides exhibit excellent temperature stability. For applications that require stability in extreme temperature conditions the RPF TTD substrate can be temperature controlled by thermoelectric elements.

The proposed device can also function as an encoder–decoder for wavelength CDMA. It converts optical pulses into time-stretched coded bit streams for which each 1 (a chip) is at a different optical wavelength. The input pulse that has a spectral width identical to the free spectral range of the RPF will be coded into a bit stream with each chip at a unique wavelength as determined by the delay in each recirculating feedback path. By incorporating switchable path lengths into each wavelength feedback path one can achieve arbitrary chip positions that correspond to individual code sequences. The code weight, corresponding to the total number of chips in the code, is fixed by the number of wavelength channels in the RPF. Thus each data bit is coded in both optical wavelength and time domains. Multidimensional (wavelength and time) CDMA significantly enhances network security and facilitates simultaneous communication among a large number of nodes.[3] A similar filter with inverted wavelength-delay length mapping functions as a matched filter in the receive mode. It produces a perfect autocorrelation with zero sidelobes for arbitrary CDMA coding patterns in wavelength and time domains.

In conclusion, we have demonstrated a recirculating photonic filter that can realize time delay for applications in phased-array antenna feeds and optical CDMA coders–decoders. A monolithic device with integrated feedback delay lines with as many as 64 wavelength channels seems achievable with current silica-waveguide technology.[4]

## References

1. A. J. Mendez, J. L. Lambert, J. M. Morookian, and R. M. Gagliardi, IEEE Photon. Technol. Lett. **6**, 1146 (1994).
2. E. Park, A. J. Mendez, and E. Garmire, IEEE Photon. Technol. Lett. **4**, 1160 (1992).
3. L. Tancevski, I. Andonovic, and J. Budin, IEEE Photon. Technol. Lett. **7**, 573 (1995).
4. K. Okamoto, K. Moriwaki, and S. Suzuki, Electron. Lett. **31**, 184 (1995).
5. L. J. Lembo, T. Holcomb, M. Wickham, P. Wisseman, and J. C. Brock, Proc. SPIE **2155**, 13 (1994).
6. W. Ng, R. Loo, V. Jones, and J. Lewis, in *Digest of the LEOS Summer Topical Meeting on RF Optoelectronics* (Institute of Electrical and Electronics Engineers, New York, 1995), p. 39.

# DISTRIBUTION LIST

| addresses | number of copies |
|---|---|
| AIR FORCE RESEARCH LABORATORY/SNDR<br>JAMES HUNTER<br>25 ELECTRONIC PKY<br>ROME NY 13441-4515 | 10 |
| REGENTS OF THE UNIVERSITY OF CA<br>UNIVERSITY OF CA LOS ANGELES<br>10945 LECONTE AVE 1400 PVUB<br>LOS ANGELES CA 90095-1406 | 5 |
| AFRL/IFOIL<br>TECHNICAL LIBRARY<br>26 ELECTRONIC PKY<br>ROME NY 13441-4514 | 1 |
| ATTENTION: DTIC-OCC<br>DEFENSE TECHNICAL INFO CENTER<br>8725 JOHN J. KINGMAN ROAD, STE 0944<br>FT. BELVOIR, VA 22060-6218 | 1 |
| DEFENSE ADVANCED RESEARCH<br>PROJECTS AGENCY<br>3701 NORTH FAIRFAX DRIVE<br>ARLINGTON VA 22203-1714 | 1 |
| ATTN: NAN PFRIMMER<br>IIT RESEARCH INSTITUTE<br>201 MILL ST.<br>ROME, NY 13440 | 1 |
| AFIT ACADEMIC LIBRARY<br>AFIT/LDR, 2950 P.STREET<br>AREA B, BLDG 642<br>WRIGHT-PATTERSON AFB OH 45433-7765 | 1 |
| AFRL/MLME<br>2977 P STREET, STE 6<br>WRIGHT-PATTERSON AFB OH 45433-7739 | 1 |

```
ATTN:  SMDC IM PL                                    1
US ARMY SPACE & MISSILE DEF CMD
P.O. BOX 1500
HUNTSVILLE AL 35807-3801


TECHNICAL LIBRARY D0274(PL-TS)                       1
SPAWARSYSCEN
53560 HULL ST.
SAN DIEGO  CA  92152-5001


COMMANDER, CODE 4TL000D                              1
TECHNICAL LIBRARY, NAWC-WD
1 ADMINISTRATION CIRCLE
CHINA LAKE  CA  93555-6100


CDR, US ARMY AVIATION & MISSILE CMD                  2
REDSTONE SCIENTIFIC INFORMATION CTR
ATTN: AMSAM-RD-OB-R, (DOCUMENTS)
REDSTONE ARSENAL AL 35898-5000


REPORT LIBRARY                                       1
MS P364
LOS ALAMOS NATIONAL LABORATORY
LOS ALAMOS NM 87545


AFIWC/MSY                                            1
102 HALL BLVD, STE 315
SAN ANTONIO TX 78243-7016


USAF/AIR FORCE RESEARCH LABORATORY                   1
AFRL/VSOSA(LIBRARY-BLDG 1103)
5 WRIGHT DRIVE
HANSCOM AFB  MA  01731-3004


ATTN:  EILEEN LADUKE/D460                            1
MITRE CORPORATION
202 BURLINGTON RD
BEDFORD MA 01730


OUSD(P)/DTSA/DUTD                                    1
ATTN:  PATRICK G. SULLIVAN, JR.
400 ARMY NAVY DRIVE
SUITE 300
ARLINGTON VA 22202
```

AIR FORCE RESEARCH LAB/SND                    1
25 ELECTRONIC PKY
ROME NY  13441-4515


JOANNE L. ROSSI                               1
AIR FORCE RESEARCH LAB/SNW
25 ELECTRONIC PKY
ROME NY  13441-4515


ROBERT T. KEMERLEY                            1
AIR FORCE RESEARCH LABORATORY/SND
2241 AVIONICS CIRCLE, RM C2G69
WRIGHT-PATTERSON AFB OH 45433-7322